

# The Polarized and Unpolarized Photon Content of the Nucleon

M. Glück, C. Pisano, E. Reya

*Universität Dortmund, Institut für Physik,  
D-44221 Dortmund, Germany*

## Abstract

The equivalent photon content of polarized and unpolarized nucleons (protons, neutrons), utilized in Weizsäcker–Williams approximations, are presented. For this purpose a new expression for the elastic photon component of a polarized nucleon is derived. The inelastic photon components are obtained from the corresponding momentum evolution equations subject to the boundary conditions of their vanishing at some low momentum scale. The resulting photon asymmetries, important for estimating cross section asymmetries in photon induced subprocesses are also presented for some typical relevant momentum scales.

The concept of the photon content of (charged) fermions is based on the equivalent photon (Weizäcker–Williams) approximation [1]. Applied to the nucleon  $N = p, n$  it consists of two parts, an elastic one due to  $N \rightarrow \gamma N$  and an inelastic part due to  $N \rightarrow \gamma X$  with  $X \neq N$ . Accordingly the total photon distribution of the nucleon is given by

$$\gamma(y, Q^2) = \gamma_{el}(y) + \gamma_{inel}(y, Q^2) \quad (1)$$

where the elastic contribution of the proton,  $\gamma_{el}^p$ , has been presented in [2] which can be generally written as

$$\gamma_{el}(y) = -\frac{\alpha}{2\pi} \int_{t_{\min}}^{t_{\max}} \frac{dt}{t} \left\{ \left[ 2 \left( \frac{1}{y} - 1 \right) + \frac{2m^2 y}{t} \right] H_1(t) + y G_M^2(t) \right\} \quad (2)$$

where  $t \equiv q^2 = -Q^2$  and

$$H_1(t) \equiv F_1^2(t) + \tau F_2^2(t) = \frac{G_E^2(t) + \tau G_M^2(t)}{1 + \tau} \quad (3)$$

with  $\tau \equiv -t/4m^2$ ,  $m$  being the nucleon mass, and where  $G_E = F_1 - \tau F_2$  and  $G_M = F_1 + F_2$  are the common elastic (Sachs) form factors which are conveniently parametrized by the well known dipole form proportional to  $(1 - t/0.71 \text{ GeV}^2)^{-2}$  as extracted from experiment. For the proton, where  $F_1^p(0) = 1$  and  $F_2^p(0) = \kappa_p \simeq 1.79$ , we have

$$G_E^p(t) = (1 + a\tau)^{-2}, \quad G_M^p(t) \simeq \mu_p G_E^p(t), \quad H_1^p(t) = \frac{1 + \mu_p^2 \tau}{1 + \tau} (1 + a\tau)^{-4} \quad (4)$$

with  $\mu_p = 1 + \kappa_p \simeq 2.79$  and  $a \equiv 4m^2/0.71 \text{ GeV}^2 \simeq 4.96$ . For the neutron, where  $F_1^n(0) = 0$  and  $F_2^n(0) = \kappa_n \simeq -1.91$ , we have

$$G_E^n(t) = \kappa_n \tau (1 + a\tau)^{-2}, \quad G_M^n(t) = \kappa_n (1 + a\tau)^{-2}, \quad H_1^n(t) = \kappa_n^2 \tau (1 + a\tau)^{-4}. \quad (5)$$

In the relevant kinematic region  $s \gg m^2$  the integration bounds in (2) can be approximated by  $t_{\min} = -\infty$  and  $t_{\max} = -m^2 y^2 / (1 - y)$  so as to obtain an universal process independent  $\gamma_{el}(x)$ . Equation (2) can now be analytically integrated which yields for the proton

$$\gamma_{el}^p(y) = \frac{\alpha}{2\pi} \frac{2}{y} \left\{ \left[ 1 - y + \frac{y^2}{4} (1 + 4a + \mu_p^2) \right] I + (\mu_p^2 - 1) \left[ 1 - y + \frac{y^2}{4} \right] \tilde{I} - \frac{1 - y}{z^3} \right\} \quad (6)$$

and for the neutron

$$\gamma_{el}^n(y) = \frac{\alpha}{2\pi} \kappa_n^2 \frac{y}{2} \left\{ I + \frac{1}{3} \frac{1}{(z-1)z^3} \right\} \quad (7)$$

where  $z \equiv 1 + \frac{a}{4} \frac{y^2}{1-y}$  and

$$I = \int_{\frac{y^2}{4(1-y)}}^{\infty} d\tau \frac{1}{\tau(1+a\tau)^4} = -\ln \left( 1 - \frac{1}{z} \right) - \frac{1}{z} - \frac{1}{2z^2} - \frac{1}{3z^3} \quad (8)$$

$$\tilde{I} = \int_{\frac{y^2}{4(1-y)}}^{\infty} d\tau \frac{1}{(1+\tau)(1+a\tau)^4} = -\frac{1}{a_-^4} \ln \left( 1 + \frac{a_-}{z} \right) + \frac{1}{a_-^3 z} - \frac{1}{2a_-^2 z^2} + \frac{1}{3a_- z^3} \quad (9)$$

with  $a_- = a - 1$ . For arriving at (6) we have also utilized the relation

$$\int_{\frac{y^2}{4(1-y)}}^{\infty} d\tau \frac{1}{\tau^2(1+a\tau)^4} = -4aI + 4\frac{1-y}{y^2 z^3}$$

which will be also relevant for the polarized photon contents to be presented below. Our result in (6) agrees with the one presented in a somewhat different form in [2]. Finally, the inelastic part in (1) has been given in [3],

$$\frac{d\gamma_{inel}^N(y, Q^2)}{d \ln Q^2} = \frac{\alpha}{2\pi} \sum_{q=u,d,s} e_q^2 \int_y^1 \frac{dx}{x} P_{\gamma q} \left( \frac{y}{x} \right) [q^N(x, Q^2) + \bar{q}^N(x, Q^2)] \quad (10)$$

with  $P_{\gamma q}(x) = [1 + (1-x)^2]/x$  and where  $q^p \equiv \bar{q}^{(-)}$  and  $u^n = \bar{d}^{(-)}$ ,  $d^n = \bar{u}^{(-)}$ ,  $s^n = \bar{s}^{(-)}$ . This equation was integrated subject to the ‘minimal’ boundary condition  $\gamma_{inel}^N(y, Q_0^2) = 0$  at [4]  $Q_0^2 = 0.26 \text{ GeV}^2$ , which is obviously not compelling and affords further theoretical and experimental studies. Since for the time being there are no experimental measurements available, the ‘minimal’ boundary condition provides at present a rough estimate for the inelastic component at  $Q^2 \gg Q_0^2$ .

Clearly, the nucleon’s photon content  $\gamma^N(x, Q^2)$  is not such a fundamental quantity as are its underlying parton distributions  $f(x, Q^2) = q, \bar{q}, g$  or the parton distributions  $f^\gamma(x, Q^2)$  of the photon, since  $\gamma^p(x, Q^2)$  is being derived from these more fundamental quantities. It represents mainly a technical device which allows for a simpler and more efficient calculation of photon-induced subprocesses. For example, the analysis of the

deep inelastic Compton scattering process  $ep \rightarrow e\gamma X$  reduces [3, 5] to the calculation of the  $2 \rightarrow 2$  subprocess  $e\gamma \rightarrow e\gamma$  instead of having to calculate the full  $2 \rightarrow 3$  subprocess  $eq \rightarrow e\gamma q$ . Similar remarks hold for the production of charged heavy particles (e.g. Higgses) via  $\gamma\gamma$  fusion at high energy  $pp$  colliders,  $pp \rightarrow \gamma\gamma X \rightarrow H^+ H^- X$ . The reliability of this approximation remains, however, to be studied.

Our main purpose here is to extend these calculations to the polarized sector, i.e., to

$$\Delta\gamma(y, Q^2) = \Delta\gamma_{el}(y) + \Delta\gamma_{inel}(y, Q^2). \quad (11)$$

The inelastic contribution derives from a straightforward extension of eq. (10),

$$\frac{d\Delta\gamma_{inel}^N(y, Q^2)}{d\ln Q^2} = \frac{\alpha}{2\pi} \sum_{q=u,d,s} e_q^2 \int_y^1 \frac{dx}{x} \Delta P_{\gamma q}\left(\frac{y}{x}\right) [\Delta q^N(x, Q^2) + \Delta \bar{q}^N(x, Q^2)] \quad (12)$$

where  $\Delta P_{\gamma q}(x) = [1 - (1-x)^2]/x = 2-x$ . We integrate this evolution equation assuming again the not necessarily compelling ‘minimal’ boundary condition  $\Delta\gamma_{inel}^N(y, Q_0^2) = 0$ , according to  $|\Delta\gamma_{inel}(y, Q_0^2)| \leq \gamma_{inel}(y, Q_0^2) = 0$ , at  $Q_0^2 = 0.26 \text{ GeV}^2$  using the recent LO polarized parton densities of [6].

The elastic distribution  $\Delta\gamma_{el}(y)$  in (11) is determined via the antisymmetric part of the tensor describing the photon emitting fermion (nucleon)

$$T^{\mu\nu} = Tr \left[ \frac{1}{2} (1 + \gamma_5 \not{n}) (\not{p} + m) \Gamma^\mu (\not{p}' + m) \Gamma^\nu \right] \quad (13)$$

for the generic process

$$N(p; n) + a(k; s) \rightarrow N(p') + X \quad (14)$$

where  $a$  being a suitable target (parton, photon, etc.) with momentum  $k$  and  $n, s$  are the appropriate polarization vectors [7] satisfying  $n \cdot p = 0$  and  $s \cdot k = 0$ . In terms of the Dirac and Pauli form factors  $F_{1,2}(t)$  of the nucleon the elastic vertices  $\Gamma^\mu$  are given by

$$\Gamma^\mu = (F_1 + F_2) \gamma^\mu - \frac{1}{2m} F_2 (p + p')^\mu. \quad (15)$$

The analysis is now a straightforward extension of the calculation [7] of the polarized Weizsäcker–Williams distribution resulting from a photon emitting fermion (electron) where  $N \rightarrow e$  in (14) with  $\Gamma^\mu = \gamma^\mu$ , and all relevant definitions and kinematics can be found in [7] as well. The resulting antisymmetric part <sup>1</sup> of  $T^{\mu\nu}$  is

$$T_A^{\mu\nu} = 2im G_M^2 \varepsilon^{\mu\nu\rho\sigma} n_\rho q_\sigma + 2i G_M (F_2/2m) \left[ (p+p')^\mu \varepsilon^{\nu\rho\sigma\sigma'} - (p+p')^\nu \varepsilon^{\mu\rho\sigma\sigma'} \right] n_\rho p_\sigma p'_{\sigma'} \quad (16)$$

with  $q = p - p'$ . It is now straightforward to contract  $T_A^{\mu\nu}$  with the appropriate antisymmetric part of the tensor  $W_A^{\mu\nu}$  describing the polarized target  $a(k; s)$  in (14) which is expressed in terms of the usual polarized structure functions  $g_1$  and  $g_2$  where all terms proportional to  $g_2$  drop in  $T_A \cdot W_A$ . This yields

$$\begin{aligned} \Delta\gamma_{el}(y) &= -\frac{\alpha}{2\pi} \int_{t_{\min}}^{t_{\max}} \frac{dt}{t} \left\{ \left[ 2 - y + \frac{2m^2 y^2}{t} \right] G_M^2(t) - 2 \left[ 1 - y + \frac{m^2 y^2}{t} \right] G_M(t) F_2(t) \right\} \\ &= -\frac{\alpha}{2\pi} \int_{t_{\min}}^{t_{\max}} \frac{dt}{t} G_M(t) \left\{ \left[ 2 - y + \frac{2m^2 y^2}{t} \right] F_1(t) + y F_2(t) \right\} \end{aligned} \quad (17)$$

with  $y = k \cdot q / k \cdot p$  and the first term proportional to  $G_M^2$  in the first line corresponds to the pointlike result of [7]. Following [2], we again approximate the integration bounds by  $t_{\min} = -\infty$  and  $t_{\max} = -m^2 y^2 / (1 - y)$  as in (2) in order to obtain an universal process independent polarized elastic distribution. Using, in addition to (4) and (5),

$$F_1^p(t) = \frac{1 + \mu_p \tau}{1 + \tau} (1 + a\tau)^{-2}, \quad F_2^p(t) = \frac{\kappa_p}{1 + \tau} (1 + a\tau)^{-2} \quad (18)$$

$$F_1^n(t) = 2\kappa_n \frac{\tau}{1 + \tau} (1 + a\tau)^{-2}, \quad F_2^n(t) = \kappa_n \frac{1 - \tau}{1 + \tau} (1 + a\tau)^{-2}, \quad (19)$$

---

<sup>1</sup>It should be noted that the symmetric (unpolarized) tensor

$$\begin{aligned} T_S^{\mu\nu} &= Tr[(\not{p} + m)\Gamma^\mu(\not{p}' + m)\Gamma^\nu] \\ &= 4G_M^2 \left[ p^\mu p'^\nu + p'^\mu p^\nu + \frac{q^2}{2} g^{\mu\nu} \right] - 4(p+p')^\mu (p+p')^\nu \left[ G_M F_2 - \frac{1}{2} \left( 1 - \frac{q^2}{4m^2} \right) F_2^2 \right] \end{aligned}$$

gives rise to the same Weizsäcker–Williams distribution obtained in a somewhat less transparent way in [2], i.e. to eq. (2), when the analysis [8] for a photon emitting pointlike unpolarized fermion (electron) is straightforwardly extended to an unpolarized nucleon,  $N(p) + a(k) \rightarrow N(p') + X$ , instead to the polarized process (14).

eq. (17) yields for the proton

$$\Delta\gamma_{el}^p(y) = \frac{\alpha}{2\pi} \mu_p \left\{ \left[ (2-y) \left( 1 + \kappa_p \frac{y}{2} \right) + 2ay^2 \right] I + 2\kappa_p \left( 1 - y + \frac{y^2}{4} \right) \tilde{I} - 2 \frac{1-y}{z^3} \right\}, \quad (20)$$

and for the neutron

$$\Delta\gamma_{el}^n(y) = \frac{\alpha}{2\pi} \kappa_n^2 \left\{ y(1-y)I + 4\left(1-y + \frac{y^2}{4}\right)\tilde{I} \right\} \quad (21)$$

with  $I$  and  $\tilde{I}$  being given in (8) and (9). These latter two equations together with (12) for  $N = p, n$  yield now the total photon content  $\Delta\gamma^N(y, Q^2)$  of a polarized nucleon in (11).

Our results for  $\Delta\gamma^p(y, Q^2)$  in (11) are shown in fig. 1 for some typical values of  $Q^2$  up to  $Q^2 = M_W^2 = 6467 \text{ GeV}^2$ . For comparison the expectations for the unpolarized  $\gamma^p(y, Q^2)$  in (1) are depicted as well. The  $Q^2$ -independent polarized and unpolarized elastic contributions in eq. (20) and (6), respectively, are also shown separately. Due to the singular small- $x$  behavior of the unpolarized parton distributions  $x \bar{q}^{(-)}(x, Q^2)$  in (10) as well as of the singular  $y\gamma_{el}^p(y)$  in (6) as  $y \rightarrow 0$ , the total  $y\gamma^p(y, Q^2)$  in fig. 1 increases as  $y \rightarrow 0$ , whereas the polarized  $y\Delta\gamma^p(y, Q^2) \rightarrow 0$  as  $y \rightarrow 0$  because of the vanishing of the polarized parton distributions  $x\Delta \bar{q}^{(-)}(x, Q^2)$  in (12) at small  $x$  and of the vanishing  $y\Delta\gamma_{el}^p(y)$  in (20) at small  $y$ . In fact,  $y\Delta\gamma^p(y, Q^2)$  is negligibly small for  $y \lesssim 10^{-3}$  as compared to  $y\gamma^p(y, Q^2)$ . For larger values of  $y$ ,  $y > 10^{-2}$ ,  $y\Delta\gamma^p(y, Q^2)$  becomes sizeable and in particular is dominated by the  $Q^2$ -independent elastic contribution  $y\Delta\gamma_{el}^p(y)$  at moderate values of  $Q^2$ ,  $Q^2 \lesssim 100 \text{ GeV}^2$  (with a similar behavior in the unpolarized sector). This is evident from fig. 2 where the results of fig. 1 are plotted versus a linear  $y$  scale. The asymmetry  $A_\gamma^p(y, Q^2)$  is shown in fig. 3 where

$$A_\gamma(y, Q^2) \equiv [\Delta\gamma_{el}(y) + \Delta\gamma_{inel}(y, Q^2)] / \gamma(y, Q^2) \quad (22)$$

with the total unpolarized photon content of the nucleon being given by (1). To illustrate the size of  $\Delta\gamma_{el}^p$  relative to the unpolarized  $\gamma_{el}^p$ , we also show the  $Q^2$ -independent ratio  $\Delta\gamma_{el}^p(y)/\gamma_{el}^p(y)$  in fig. 3 which approaches 1 as  $y \rightarrow 1$ .

The polarized photon distributions  $\Delta\gamma^p(y, Q^2)$  shown thus far always refer to the so called ‘valence’ scenario [6] where the polarized parton distributions in (12) have flavor–broken light sea components  $\Delta\bar{u} \neq \Delta\bar{d} \neq \Delta\bar{s}$ , as is the case (as well as experimentally required) for the unpolarized ones in (10) where  $\bar{u} \neq \bar{d} \neq \bar{s}$ . Using instead the somehow unrealistic ‘standard’ scenario [6] for the polarized parton distributions with a flavor–unbroken sea component  $\Delta\bar{u} = \Delta\bar{d} = \Delta\bar{s}$ , all results shown in figs. 1–3 remain practically almost undistinguishable. The same holds true for the photon content of a polarized neutron to which we now turn.

The results for  $\Delta\gamma^n(y, Q^2)$  are shown in fig. 4 which are sizeably smaller than the ones for the photon in fig. 1 and, furthermore, the elastic contribution is dominant while the inelastic ones become marginal at  $y \gtrsim 0.2$ . For comparison the unpolarized  $\gamma^n(y, Q^2)$  in (1) is shown in fig. 4 as well. Here,  $\gamma_{el}^n$  in (7) is marginal and  $y\gamma_{el}^n(y)$  is non–singular as  $y \rightarrow 0$  with a limiting value  $y\gamma_{el}^n(y)/\alpha = \kappa_n^2/(3\pi a) \simeq 0.078$ . Thus the increase of  $y\gamma^n(y, Q^2)$  at small  $y$  is entirely caused by inelastic component  $y\gamma_{inel}^n(y, Q^2)$  in (10), due to the singular small– $x$  behavior of  $x\bar{q}^{(-)}(x, Q^2)$ , which is in contrast to  $y\gamma^p(y, Q^2)$  in fig. 1. These facts are more clearly displayed in fig. 5 where the results of fig. 4 are presented for a linear  $y$  scale. Notice that again the polarized  $y\Delta\gamma^n(y, Q^2) \rightarrow 0$  as  $y \rightarrow 0$  because of the vanishing of the polarized parton distributions  $x\Delta\bar{q}^{(-)}(x, Q^2)$  in (12) at small  $x$  and of the vanishing of  $y\Delta\gamma_{el}^n(y)$  in (21) at small  $y$ . Finally, the asymmetry  $A_\gamma^n(y, Q^2)$  defined in (22) is shown in fig. 6 which is entirely dominated by the elastic contribution for  $x \gtrsim 0.2$ . As in fig. 3 we illustrate the size of the elastic  $\Delta\gamma_{el}^n(y)$  relative to the unpolarized  $\gamma_{el}^n(y)$  by showing the ratio  $\Delta\gamma_{el}^n/\gamma_{el}^n$  in fig. 6 as well. Notice that  $\Delta\gamma_{el}^n/\gamma_{el}^n \rightarrow \frac{6}{7}$  as  $y \rightarrow 1$  in contrast to the case of the proton.

As mentioned at the beginning the knowledge of the unpolarized photon content of the nucleon  $\gamma^N(y, Q^2)$  allows for a simpler and more efficient calculation of photon–induced subprocesses in elastic and deep inelastic  $ep$  and purely hadronic ( $pp, \dots$ ) reactions [2, 3, 5, 9, 10, 11, 12]. For example, to consider just the simple  $2 \rightarrow 2$  sub-

process  $e\gamma \rightarrow e\gamma$  for the analysis of the deep inelastic Compton process  $ep \rightarrow e\gamma X$  or  $e\gamma \rightarrow \nu W$  for associated  $\nu W$  production in  $ep \rightarrow \nu W X$ . Similarly, the  $\gamma\gamma$  fusion process  $\gamma\gamma \rightarrow \ell^+\ell^-, c\bar{c}, H^+H^-, \tilde{\ell}^+\tilde{\ell}^-, \dots$  for (heavy) lepton ( $\ell$ ), heavy quark ( $c$ ), charged Higgs ( $H^\pm$ ) and slepton ( $\tilde{\ell}$ ) production etc. can be easily analyzed in purely hadronic  $pp$  reactions which is also an interesting possibility of producing charged particles which do not have strong interactions. In particular the  $\gamma\gamma \rightarrow \mu^+\mu^-$  channel will give access to experimental measurements of  $\gamma^N(y, Q^2 = M_{\mu^+\mu^-}^2)$  at  $pp$ ,  $pd$  and  $dd$  colliders.

Analogous remarks hold for the longitudinally polarized  $\vec{e}\vec{N}$  and  $\vec{p}\vec{p}, \vec{p}\vec{d}$  and  $\vec{d}\vec{d}$  reactions where the polarized photon content of the nucleon  $\Delta\gamma^N(y, Q^2)$ , as calculated and studied in this article, enters. Very interestingly, it remains to be seen whether ongoing experiments at RHIC(BNL) for dimuon production,  $\vec{p}\vec{p}, \vec{d}\vec{d} \rightarrow \mu^+\mu^- X$ , can directly delineate and test our predictions for  $\Delta\gamma^N(y, M_{\mu^+\mu^-}^2)$ .

A FORTRAN package (grids) containing our results for  $\Delta\gamma^N(y, Q^2)$  as well as those for  $\gamma^N(y, Q^2)$  can be obtained by electronic mail.

This work has been supported in part by the ‘Bundesministerium für Bildung und Forschung’, Berlin/Bonn.



## References

- [1] C.F. Weizsäcker, *Z. Phys.* **88** (1934) 612;  
E.J. Williams, *Phys. Rev.* **45** (1934) 729 (L).
- [2] B.A. Kniehl, *Phys. Lett.* **B254** (1991) 267.
- [3] M. Glück, M. Stratmann, and W. Vogelsang, *Phys. Lett.* **B343** (1995) 399.
- [4] M. Glück, E. Reya, and A. Vogt, *Eur. Phys. J.* **C5** (1998) 461.
- [5] A. De Rujula and W. Vogelsang, *Phys. Lett.* **B451** (1999) 437.
- [6] M. Glück, E. Reya, M. Stratmann, and W. Vogelsang, *Phys. Rev.* **D63** (2001) 094005.
- [7] D. de Florian and S. Frixione, *Phys. Lett.* **B457** (1999) 236.
- [8] S. Frixione, M.L. Mangano, P. Nason, and G. Ridolfi, *Phys. Lett.* **B319** (1993) 339.
- [9] M. Drees and D. Zeppenfeld, *Phys. Rev.* **D39** (1989) 2536.
- [10] J. Blümlein, G. Levman, and H. Spiesberger, *J. Phys.* **G19** (1993) 1695.
- [11] M. Drees, R.M. Godbole, M. Nowakowski and S.D. Rindani, *Phys. Rev.* **D50** (1994) 2335;  
J. Ohnemus, T.F. Walsh and P.M. Zerwas, *Phys. Lett.* **B328** (1994) 369.
- [12] C.E. Carlson and K.E. Lassila, *Phys. Lett.* **97B** (1980) 291.

## Figure Captions

**Fig. 1.** The polarized and unpolarized total photon contents of the proton,  $\Delta\gamma^p$  and  $\gamma^p$ , according to eqs. (1) and (11) at some typical fixed values of  $Q^2$  (in  $\text{GeV}^2$ ). The  $Q^2$ -independent elastic contributions are given by eqs. (20) and (6).

**Fig. 2.** As in fig. 1 but for a linear  $y$  scale.

**Fig. 3.** The asymmetry of the polarized to the unpolarized photon content of the proton as defined in (22) at various fixed values of  $Q^2$  (in  $\text{GeV}^2$ ) according to the results in fig. 1. The  $Q^2$ -dependence of the elastic contribution to  $A_\gamma^p$  is caused by the  $Q^2$ -dependent total unpolarized photon content in the denominator of (22). For illustration the  $Q^2$ -independent elastic ratio  $\Delta\gamma_{el}^p/\gamma_{el}^p$  is shown as well.

**Fig. 4.** As fig. 1 but for the neutron, with elastic polarized and unpolarized contributions being given by eqs. (21) and (7).

**Fig. 5.** As in fig. 4 but for a linear  $y$  scale.

**Fig. 6.** As fig. 3 but for the neutron asymmetry according to the results in fig. 4.

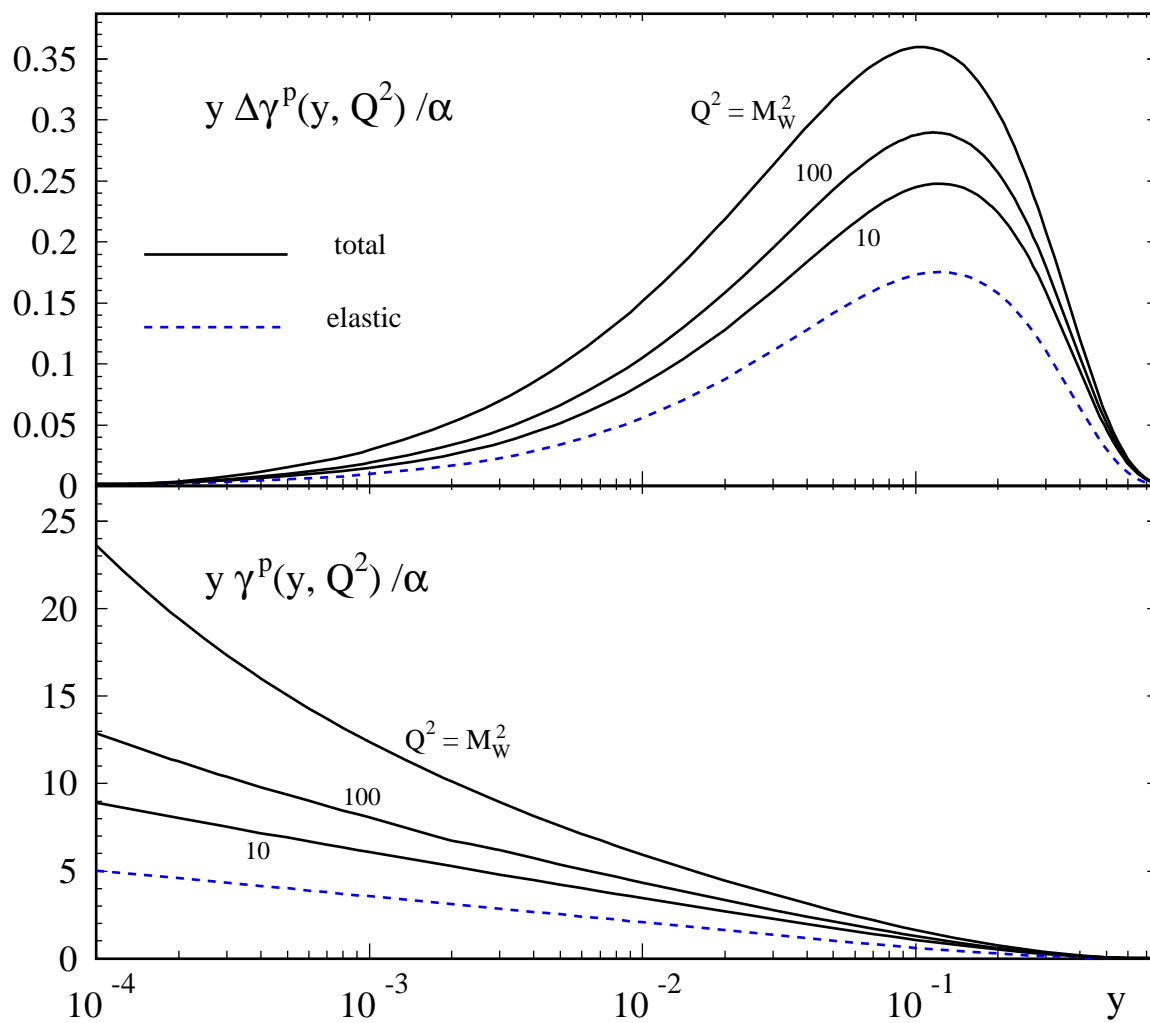


**Fig. 1**

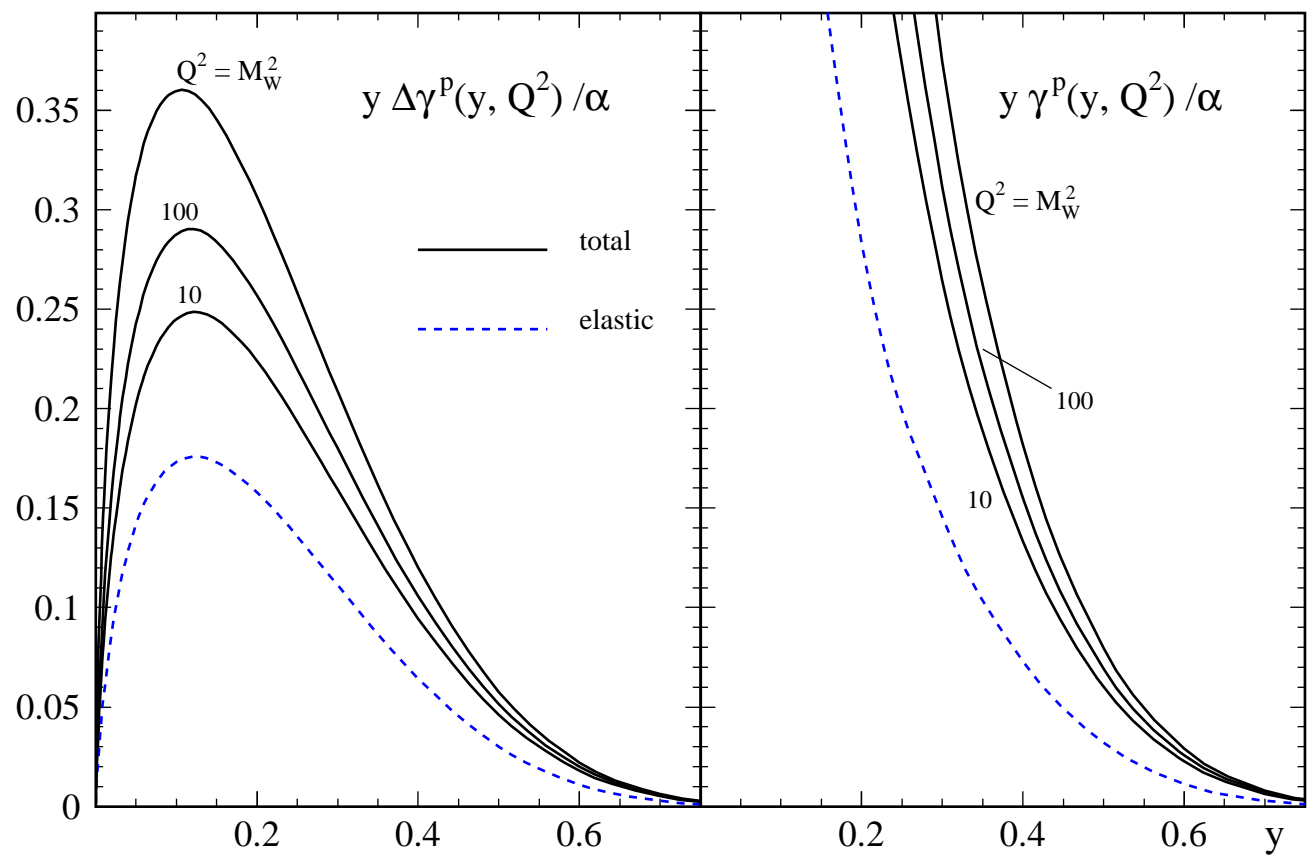


Fig. 2

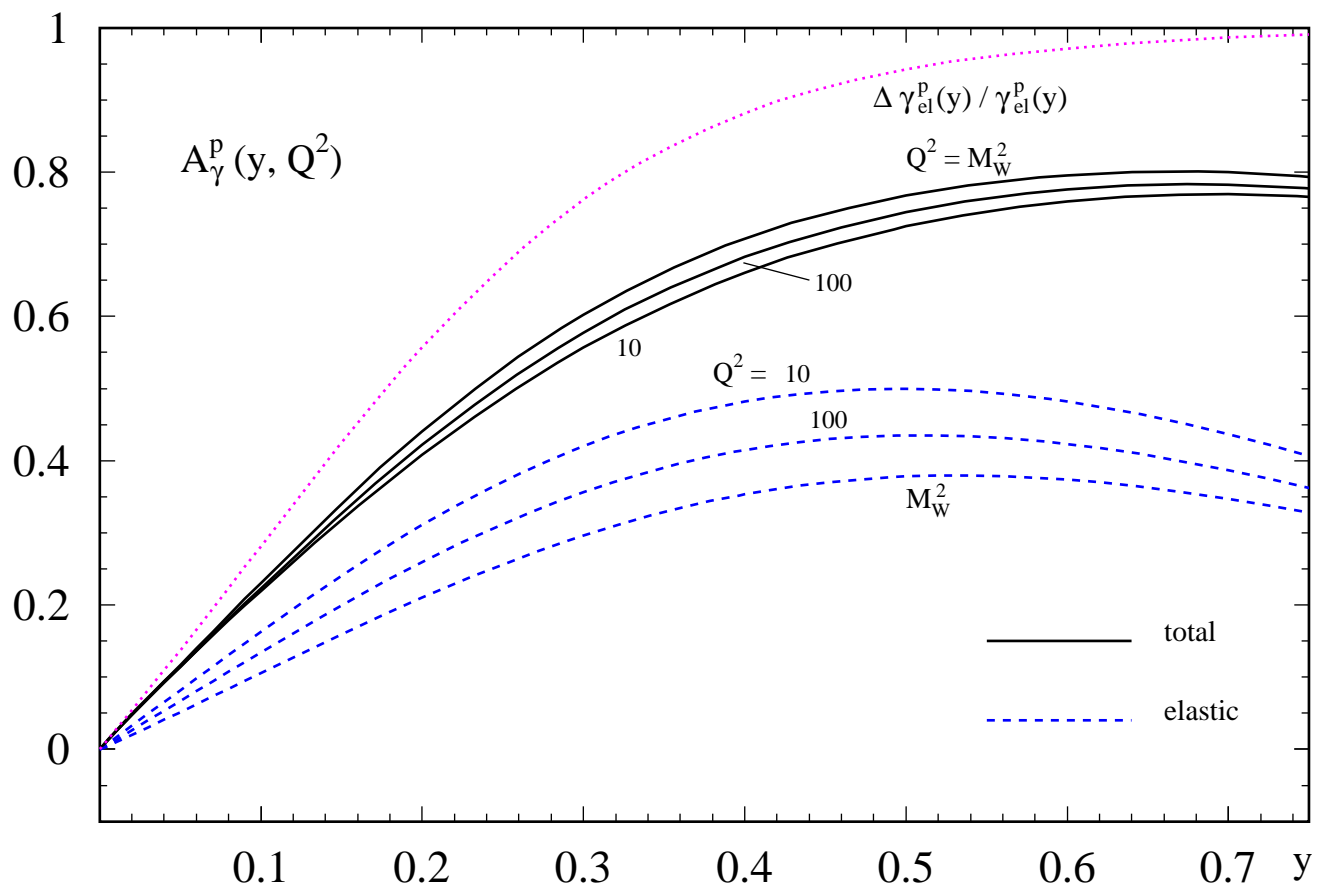


Fig. 3

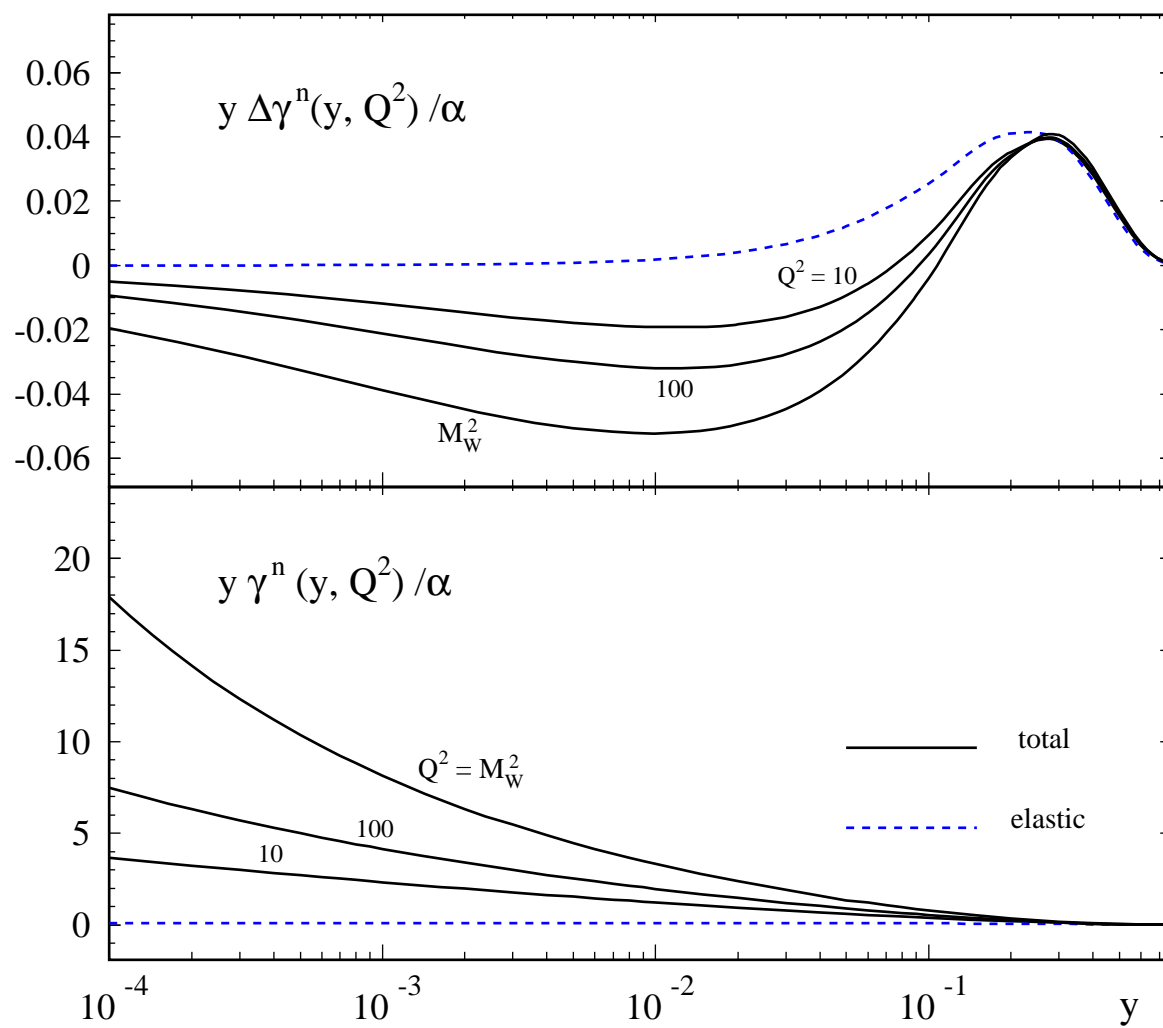


Fig. 4

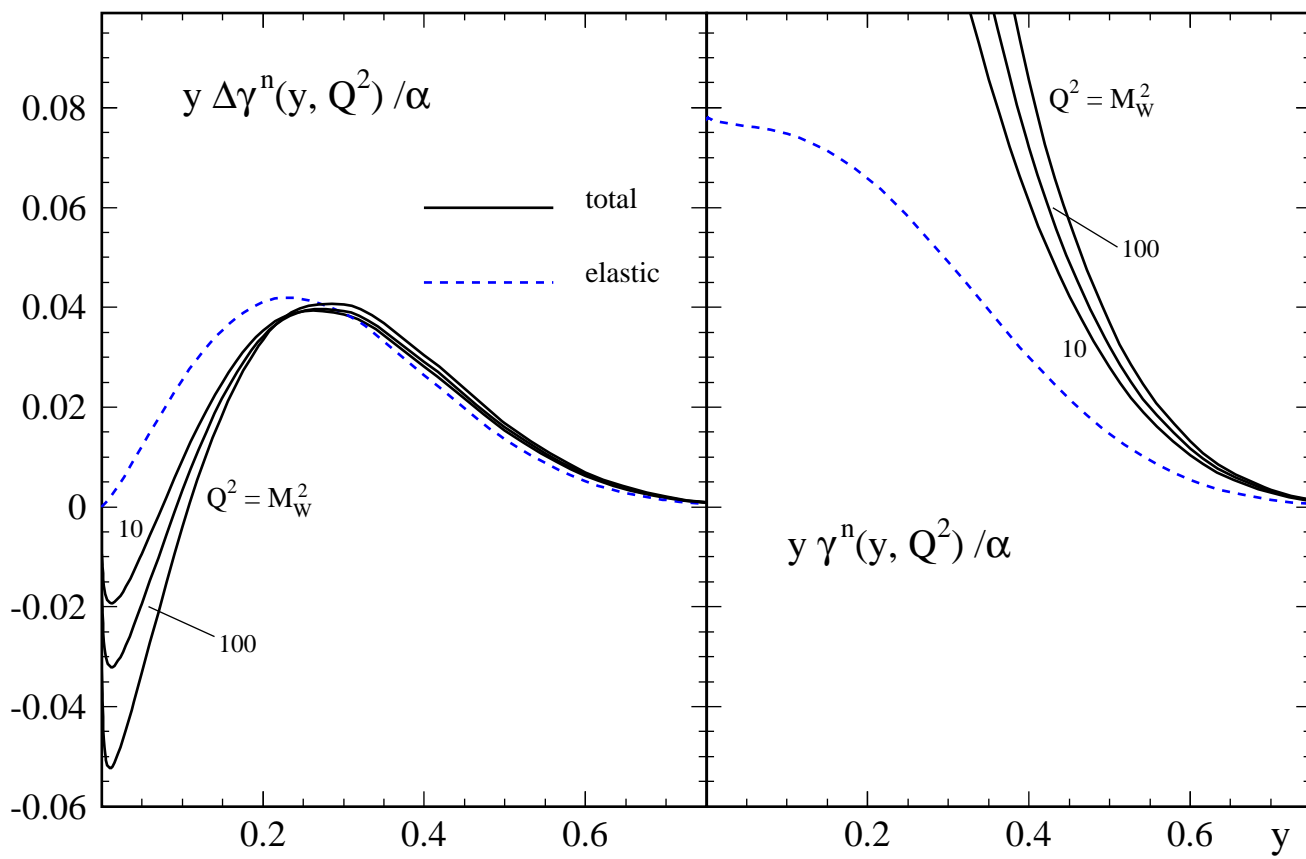


Fig. 5

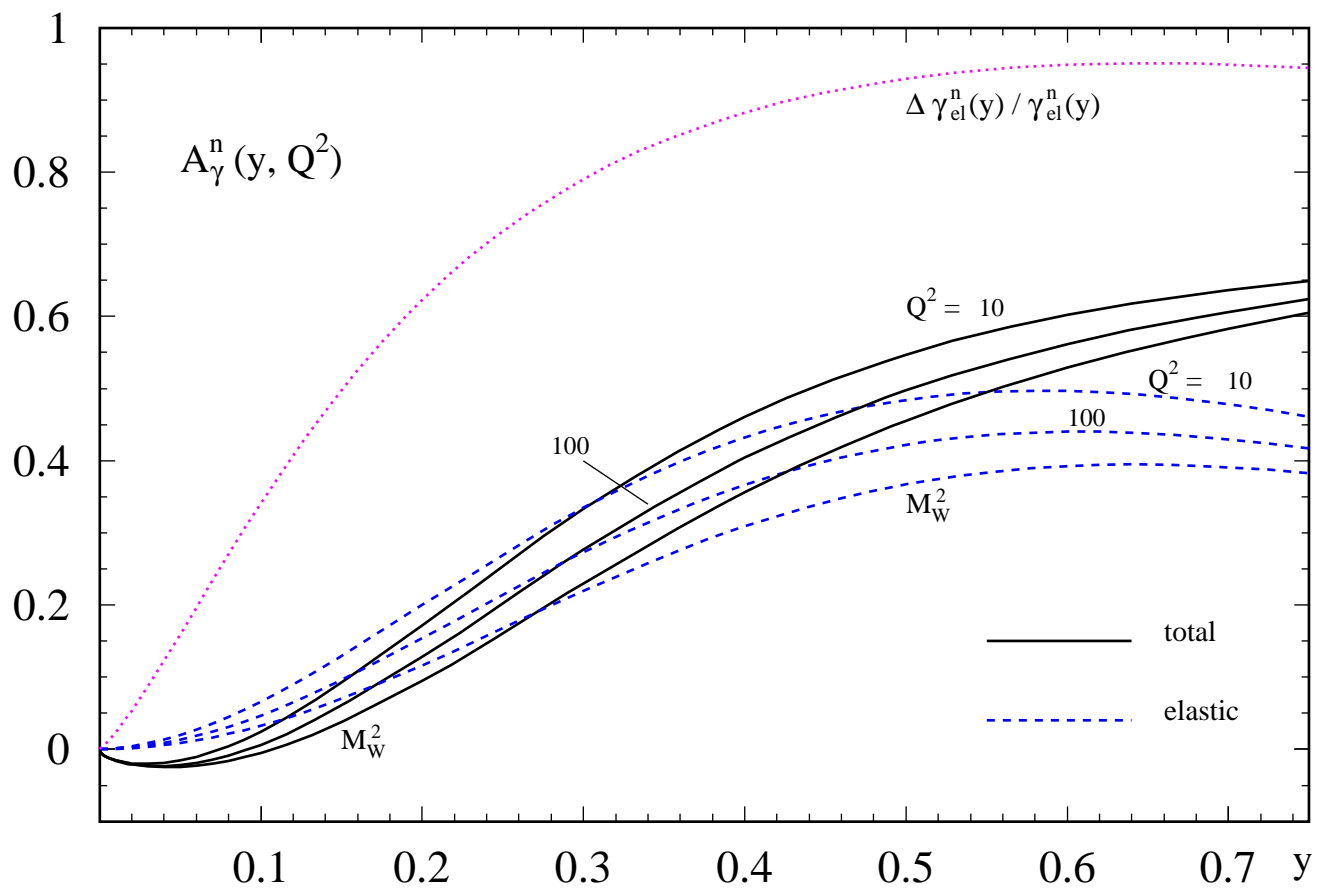


Fig. 6